In vitro toxicity studies of polymer-coated gold nanorods

Raja G. Rayavarapu[1,†], Wilma Petersen[1,†], Liesbeth Hartsuiker[2], Patrick Chin[3], Hans Janssen[4], Fijs W. B. van Leeuwen[3], Cees Otto[2], Srirang Manohar[1,‡] and Ton G. van Leeuwen[1,5]

[1]Biomedical Photonic Imaging Group, MIRA Institute for Biomedical Technology and Technical Medicine, Faculty of Science and Technology, University of Twente, P.O. Box 217, 7500AE Enschede, The Netherlands

[2]Medical Cell Biophysics, MIRA Institute for Biomedical Technology and Technical Medicine, Faculty of Science and Technology, University of Twente, P.O. Box 217, 7500AE Enschede, The Netherlands

[3]Division of Diagnostic Oncology, The Netherlands Cancer Institute, 1066 CX Amsterdam, The Netherlands

[4]Division of Cell Biology, The Netherlands Cancer Institute, 1066 CX Amsterdam, The Netherlands

[5]Biomedical Engineering and Physics, Academic Medical Center, University of Amsterdam, PO Box 22700, 1100 DE Amsterdam, The Netherlands

Abstract. We evaluated cellular responses to polymer-treated gold nanorods, which were synthesized using the standard wet-chemistry method that utilizes hexadecyltrimethylammonium bromide (CTAB). The nanorod dispersions were coated with either polystyrene sulfonate (PSS) or polyethylene glycol (PEG). Two sizes of nanorods were tested, with optical responses peaking at 628 nm and 773 nm. The cells were from mammary adenocarcinoma (SKBR3), Chinese Hamster Ovary (CHO), mouse myoblast (C2C12) and Human Leukemia (HL60) cell-lines. Their mitochondrial function following exposure to the nanorods were assessed using the MTS-assay. We found PEGylated particles to have superior biocompatibility compared with PSS-coated nanorods, which showed substantial cytotoxicity. Electron microscopy showed no cellular uptake of PEGylated particles compared with their PSS counterparts. PEGylated gold nanorods also exhibited better dispersion stability in the presence of cell growth medium; PSS-coated rods tended to flocculate or cluster. In the case of the PSS-particles, toxicity correlated with surface area across the two sizes of nanorods studied.

1. Introduction

The interaction of light with gold nanoparticles has aroused much interest in the medical field, where these particles have potential as labels for light-based imaging techniques

† These authors contributed equally.
‡ S.Manohar@utwente.nl

and as photo-induced therapeutic agents [1, 2, 3, 4]. Light interaction with gold at the nanoscale is strong due to surface plasmon resonance, which leads to intense absorption or scattering peaks in the optical spectra [5]. Gold nanorods (AuNR) are characterized by two plasmon resonant peaks in the spectra. The lower energy peak, which arises from plasmons excited along the long axis of the rod, is called the longitudinal plasmon (LP) peak and can be tuned to occur in the far-red or near-infrared (NIR) between 650 - 950 nm [5]. The transverse plasmon (TP) peak due to plasmons excited along the AuNR's short axis, remains pegged at around 520 nm.

The AuNRs' strong absorption or scattering can provide contrast for imaging using techniques such as photoacoustic imaging [6] and optical coherence tomography (OCT) [7]. Further, by optimizing the delivered light spatially and temporally, absorption by the particles can cause sufficient heating and localized temperature rise to kill cells, opening up therapeutic applications [8]. Nanorods (NRs) are ideal for applications in tissue, since light penetration is deep in the range of 700-1100 nm, as photons undergo less absorption and scattering by tissue components [9].

While much research has been done demonstrating the potential of these plasmonic nanoparticles in laboratory and pre-clinical studies, a crucial requirement for clinical translation is biocompatibility. With gold nanorods an obstacle is the toxic surfactant hexadecyltrimethylammonium bromide (CTAB) [10], which is indispensible for synthesizing particles with good yield, and size and shape control.

CTAB is used in growth solutions comprising gold salt, gold seed, silver nitrate and a weak reducing agent. Reduction of gold on the gold seed takes place, but because CTAB assisted by silver passivates certain facets of the seed particles, gold deposition occurs preferentially on the exposed tips to yield rod-shaped particles [11, 12, 13]. It has been shown earlier on a few cell-lines that repeated centrifugations and re-dispersion in water removes excess unbound CTAB and makes AuNR dispersions relatively less toxic [14, 15, 16]. However, centrifugation can strip stabilizing CTAB off the gold, which could result in aggregation of the particles. Further, it is possible that CTAB molecules can desorb from the gold surfaces, making such these particles potentially toxic.

Thus, it is necessary to treat the particles in such a way that the CTAB is either removed from the particles or that it remains encapsulated. One approach to reduce the toxicity, has been to overcoat the CTAB particles with polyelectrolyte coatings such as poly(diallyldimethylammonium chloride) (PDADMAC), poly(4-styrenesulfonic acid) (PSS), polyacrylic acid (PAA) and poly(allylamine) hydrochloride (PAH), which prevents direct interactions between cells and CTAB, and shown to reduce cell-death in certain cell-lines [17, 18]. Another approach is to PEGylate NRs, which has been shown to ameliorate cell toxicity in several cell lines [10, 14, 15, 16], by largely replacing CTAB.

We have expanded such cell-toxicity studies by applying PSS-coated and PEGylated nanorods to a number of cell lines. The cells used were SKBR3, CHO, C2C12 and HL60 cells. Cellular uptake in SKBR3 cells was also investigated using transmission electron microscopy (TEM). We studied two AuNR samples with plasmon peaks roughly

occupying opposite ends of the optical imaging and therapeutic window - 628 nm and 773 nm.

2. Materials and Methods

2.1. Gold nanorod synthesis

The following reagents were used: the gold salt (tetrachloroauric acid $HAuCl_4.3H_2O$) from Acros Organics (Belgium); hexadecyltrimethylammonium bromide (CTAB > 99%), sodium borohydride ($NaBH_4$ 99%) and ascorbic acid (99%) from Fluka (The Netherlands); silver nitrate ($AgNO_3$ 99.8%) from Merck (Germany).

Prior to use, all glassware was cleaned with 8% hydrofluoric acid (HF), further with aqua regia (HCl/HNO_3) and rinsed twice with Milli Q water.

AuNRs were synthesized using the seed-mediated method [19, 20] that requires the addition of gold seed to a growth solution with shape directing surfactant CTAB. The method is based on Ref. [21] and details of the protocol are provided in Supplementary Information. We briefly describe the steps involved here. Reducing agent $NaBH_4$ is added to gold salt and surfactant CTAB. Within a few minutes as the reaction proceeds, the pre-formed spheres are used to seed a growth solution comprising gold salt, CTAB, and $AgNO_3$, which has been primed with the weak reducing agent ascorbic acid.

Passivation of certain facets of the growing gold seed by CTAB assisted by silver [11, 12, 13] causes symmetry breaking, and gold deposition is directed to occur on the exposed tips to yield rod-shaped particles. Using different $AgNO_3$ concentrations in the growth solution allows a tuning of LP peak positions. Specifically, we used appropriate $AgNO_3$ concentrations to synthesize two batches of NRs with LP peaks at 628 and 773 nm respectively. These are henceforth referred to as samples $AuNR_{628}$ nm and $AuNR_{773}$ nm respectively. (Fig. 1(a) and Fig. 2(a))

The samples were filtered in two steps using a 5 μm filter and a 0.45 μm filter respectively to remove excess CTAB which tends to forms small crystals. This is followed by centrifugation at 10000 G for 20 minutes using a Beckman Coulter ultracentrifuge. The NR pellet from one centrifugation cycle, was dispersed in Milli Q water to give stock solutions of 100 ml volumes with concentrations of the order of 10^{11} NRs/ml.

2.2. Polymer treatment of gold nanorods

The following reagents were used: methoxy PEG-thiol (5000 MW) from Fluka (The Netherlands) and polystyrene sulfonate-Na salt (15000 MW) from PolySciences (USA).

Polystyrene Sulfonate (PSS) treatment To the NR stock solution 0.1 ml of a PSS stock (10 mg PSS in 1 ml 0.01 M NaCl) and 0.05 ml of 0.01 M NaCl solution was added with gentle vortexing, and maintained at 4°C with stirring for 24 hours. The sample was then centrifuged and the supernatant with unbound PSS was discarded, and the pellet dispersed in 2.5 ml 1X PBS.

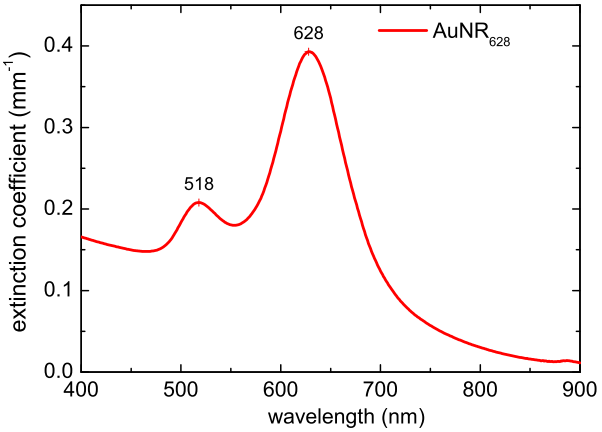

(a)

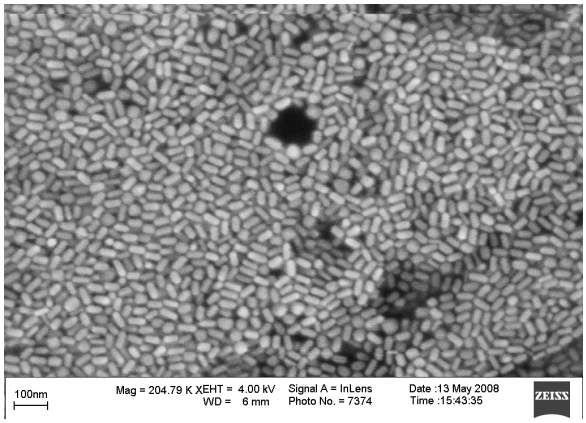

(a)

Figure 1: (a) Optical extinction spectrum of the batch of gold nanorods with longitudinal plasmon at 628 nm. The batch is designated as $AuNR_{628}$. (b) High-resolution scanning electron micrographs (SEM) of the same batch showing monodispersity of the particles.

Table 1: Average lengths, widths and aspect ratios of $AuNR_{628}$ and $AuNR_{773}$ samples derived from analysis of at least 250 particles in each case from SEM images (Fig. 1(b) and Fig 2(b)).

Sample	length (nm)	width (nm)	aspect ratio
$AuNR_{628}$	44.8 ± 2.8	18.5 ± 1.6	2.4 ± 0.2
$AuNR_{773}$	41.8 ± 3.3	11.7 ± 1.4	3.5 ± 0.4

PEG-thiol treatment The stock solution was centrifuged for a second time at 10000 G for 20 minutes, and the NR pellet dispersed in 0.5 ml of 5 mM mPEG-SH with vigorous vortexing for 20 seconds. To this, 0.5 ml of 1X PBS (Phosphate Buffer Saline) was added followed by continuous rotation for 24 hours at 4^{o}C. The resultant was subjected to two centrifugation steps to remove excess mPEG-SH from the solution and the pellet dispersed in 2.5 ml 1X PBS. [22]

2.3. Characterization

Electron microscopy of samples (Fig. 1(a) and Fig. 2(a)) was performed using the Zeiss-1550 high-resolution scanning electron microscope (SEM). Particle sizes were estimated using NI Vision module (Labview, National Instruments) on the digital SEM images with at least 250 particles considered in each sample. (See Table 1 for sizes of particles synthesized.)

Collimated transmission spectra of samples were measured using the Shimadzu PC3101 UV-Vis-NIR spectrophotometer at various stages after synthesis and polymer

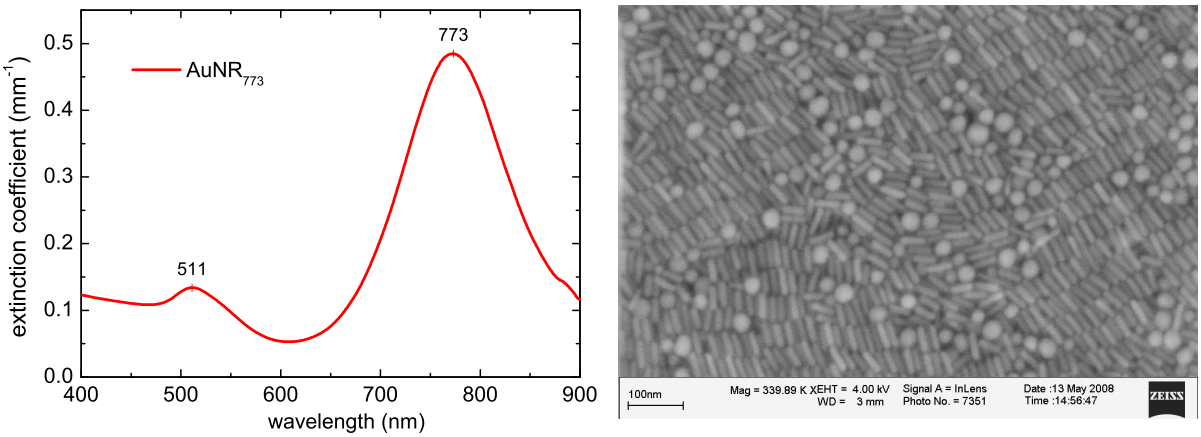

(a) (b)

Figure 2: (a) Optical extinction spectrum of batch designated as $AuNR_{773}$ showing the longitudinal plasmon peak at 773 nm. (b) High-resolution scanning electron micrographs (SEM) of the same batch showing monodispersity of the particles.

treatment. Retention of the plasmon peaks in the spectra are taken as evidence of colloidal stability following processing steps. Further, the spectra are used for estimating number densities as:

$$N = \frac{\mu_{ext}}{Q_{ext}\pi r^2}, \tag{1}$$

where, μ_{ext} is the extinction coefficient of the samples calculated from transmission data using the Beer-Lambert law (Fig. 1(a) and Fig. 2(a)), Q_{ext} is the extinction efficiency of a particle simulated using numerical methods such as the Discrete Dipole Approximation [23, 24], and r is the radius of an equivalent sphere obtained from sizes ascertained from SEM images. The concentration in number of NRs/litre is also expressed in a molar concentration in particle entities.

The zeta- (ζ-) potential of AuNRs was measured using the Malvern Zeta NS 2000 instrument (Malvern Instruments Ltd., UK). The ζ-potential serves as a criterion for inspecting surface charge changes on the nanoparticles, as well as a measure for their stability following various polymer coating steps.

2.4. Viability studies

At the moment there is no consensus on the choice of *in vitro* model systems to investigate biocompatibility of engineered nanoparticles. Our rationale for choice of cell-lines was based on the ultimate ambition that we envisage for the AuNRs that we synthesize. We wish to use AuNRs as molecular probes to obtain better photoacoustic cancer imaging [25, 26]capabilities and to implement photothermal therapeutic applications against cancer cells. SKBR3 being a human mammary adenocarcinoma cell-line was an obvious choice as clinically relevant target. In addition to human-derived cells, we also used animal-derived Chinese Hamster Ovary (CHO) and

Table 2: Start and end concentrations of nanorods in used in cell viability studies. Serial dilutions by a factor 2 are made to achieve 8 concentrations per type per batch of nanorods. The molar concentrations are in particles and not in gold atoms.

Samples	AuNR (pM)	Filtered AuNR (pM)	PSS-AuNR (pM)	PEG-AuNR (pM)
$AuNR_{628}$	20 - 0.15	20 - 0.15	174 - 1.3	165 - 1.2
$AuNR_{773}$	20 - 0.15	20 - 0.15	165 - 1.2	157 - 1.2

mouse myoblast (C2C12) cells. Finally, HL60 are human promyelocytic leukemia cells, which being rapidly dividing cells are more sensitive to toxic compounds. These are also suspension cells unlike the others which are adherent.

SKBR3 and HL60 cells were maintained using RPMI 1640 medium supplemented with glutamine, 10% FBS and 1% antibiotics (penicillin/streptomycin). CHO and C2C12 were cultured using Dulbecco's Modified Eagle's Medium (DMEM) supplemented with glucose, 10% FBS and 1% antibiotics (penicillin/streptomycin). HL60 cells were passaged every 2 days whereas the SKBR3, CHO and C2C12 cells were passaged every 3 days.

Viabilities of the cells as a response to AuNR exposure, were studied using the CellTiter 96 Aqueous Cell Proliferation Assay from Promega (The Netherlands). Viable cells can be quantified by a colorimetric change to the tetrazolium compound - MTS and an electron coupling reagent phenazine methosulfate (PMS). The MTS salt is converted into formazon by metabolically active cells [10]. The quantity of formazan product is measured by the amount of 490 nm absorbance directly from 96-well plates and is directly proportional to the number of living cells.

2.4.1. Protocol followed The adherent cells were added to specific wells of the plate to obtain approximately 5000 cells/well. The plate was equilibrated for 16 hours at 37°C in a humidified, 5% CO_2 atmosphere. HL60 cells were then dispensed into other wells to obtain approximately 5000 cells/well.

The test compounds were as-prepared, filtered, PEGylated and PSS-treated $AuNR_{628}$ and $AuNR_{773}$ rods. Each type was added in volumes of 50 μl in 8 serial dilutions (Table 2) in triplicate to the cell-line wells. The same series of dilutions in duplicate of the test materials with 50 μl medium were used without any cells as a sample background (SB) control. Culture medium (100 μl RPMI and DMEM) alone was used as a medium-only control (LC_0). The cells prepared for the assay were also used as cell-only control (LC_{100}). The plate with its well contents was maintained at 37°C in a humidified, 5% CO_2 atmosphere.

Following 24 hours exposure to the various AuNR samples, 20 μl of MTS/PMS solution was added to all the wells. The plates were wrapped in aluminum foil to prevent

exposure to light which could cause degradation of the MTS/PMS solution. The plates were incubated for a further 4 hours at 37°C in a humidified, 5% CO_2 atmosphere. The absorbance was then recorded at 490 nm using the Tecan plate reader.

2.4.2. Data processing and analysis For every dilution the average absorbance for the cells exposed in triplicate with test and assay compounds was calculated. This was corrected by deducting the average absorbance from the sample background control, and with a standard deviation (σ) calculated from a linear combination of errors [27]. As an example,

$$\langle A_{TC}\rangle_{corr} = \langle A_{TC}\rangle - \langle A_{SB}\rangle \tag{2}$$

and,

$$\sigma_{corr} = \sqrt{\sigma_{TC}^2 + \sigma_{SB}^2} \tag{3}$$

In the above, A is the absorbance, σ is the standard deviation with subscripts TC and SB representing test compound and sample background, respectively.

Further a corrected average LC_{100} absorbance is obtained by deducting average absorbance of LC_0. This is taken as absorbance associated with living cells. The percentage cell survival is calculated as:

$$\%\text{ cell survival} = \left[\frac{\langle A_{TC}\rangle}{\langle \mathrm{LC}_{100}\rangle}\right]_{corr} \times 100\% \tag{4}$$

with a corresponding standard deviation calculated as the quotient combination of errors [27], which is the fractional errors of the individual components above:

$$\sigma = \sqrt{\left(\frac{\sigma_{corr}}{\langle A_{TC}\rangle_{corr}}\right)^2 + \left(\frac{\sigma_{\mathrm{LC}_{100}}}{\langle \mathrm{LC}_{100}\rangle}\right)^2} \times \%\text{ cell survival} \tag{5}$$

The cell survival percentages are plotted as a dose-response curve which permits the calculation of the LC_{50} value which is the x-intercept of the curve at 50% cell death.

2.4.3. Electron microscopy on gold nanorod exposed cells Due to the high x-ray attenuation of AuNRs, their interaction with cells can be accurately visualized at the nm-scale using Transmission Electron Microscopy (TEM). SKBR3 cells were exposed to the three variants of $AuNR_{628}$ for 3 hours. The concentrations used were 10 pM (6×10^9 NR/ml) for PSS- and PEG-$AuNR_{628}$, and 0.1 pM (6×10^7 NR/ml) for CTAB-$AuNR_{628}$. Exposed cells were fixed in Karnovsky fixative. Post-fixation was done with 1% osmium tetroxide in 0.1 M cacodylate buffer. After washing, the pellets were stained *en bloc* with Ultrastain-1 (Leica, Vienna, Austria), followed by an ethanol dehydration series. Finally the cells were embedded in a mixture of DDSA/NMA/Embed-812 (EMS, Hatfield, USA), sectioned and stained with lead oxide and analyzed with a CM10 electron microscope (FEI, Eindhoven, the Netherlands). Only intact cells were analyzed.

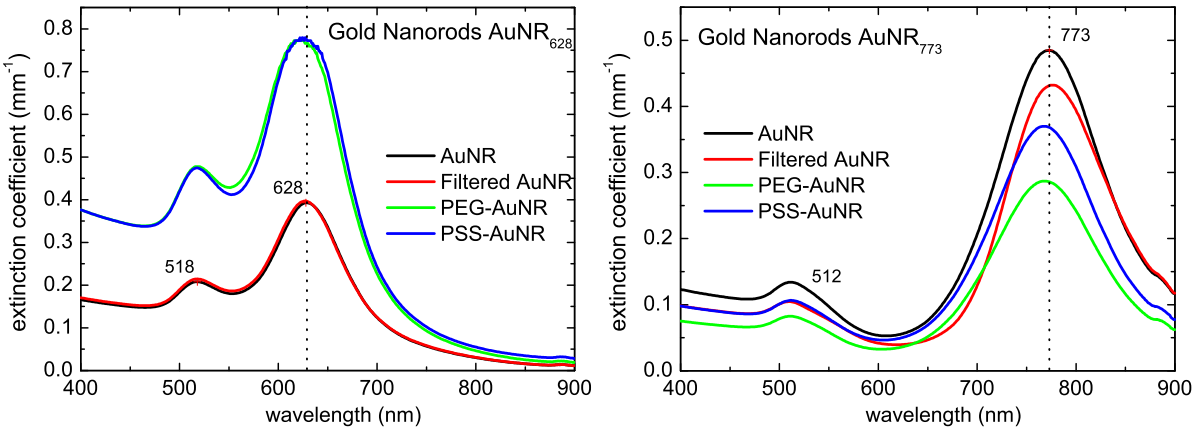

(a) (b)

Figure 3: Optical extinction spectra of gold nanorods for the conditions of as-prepared, filtered, PSS-treated and PEGylated for batches designated as (a) $AuNR_{628}$ and (b) $AuNR_{773}$. The longitudinal plasmon peak features are retained indicating that polymer-treatment has not affected colloidal stability.

Table 3: Average zeta-(ζ-) potential values of typical as-prepared and variously treated gold nanorods for the two batches. Values are seen to be nearly neutral for PEG-treated samples and negative for PSS-treated nanorods.

Samples	AuNR (mV)	Filtered AuNR (mV)	PSS-AuNR (mV)	PEG-AuNR (mV)
$AuNR_{628}$	$+37.7 \pm 3.7$	$+42.2 \pm 1.1$	-60.5 ± 1.0	-5.2 ± 0.5
$AuNR_{773}$	$+55.2 \pm 2.1$	$+58.7 \pm 3.6$	-49.6 ± 2.6	-4.1 ± 0.9

3. Results

3.1. Characterization of polymer-treated gold nanorods

Figures 3(a) and (b) are the optical extinction spectra of variously processed gold nanorods of the two batches $AuNR_{628}$ and $AuNR_{773}$. The processing is either filtration to minimize excess CTAB, PSS-treatment or PEG-treatment. The spectra of the processed particles retain the LP peaks of the as-prepared NRs, with only marginal shifts in position, indicating that particle clustering or aggregation has not taken place. These spectra also remain stable in time as tested over several months. Peak amplitude differences (Figures 3(a) and (b)) are present for the various processing steps because concentrations were not normalized at the point when the spectra were measured.

Table 3 shows the ζ-potential of various samples of the two NR types. The unprocessed and filtered AuNRs show high positive ζ-potential which is consistent with the cationic head group (CTA^+) of CTAB in the bilayer [28] on the gold surface. The PEG-AuNR show a low value of ζ-potential pointing to the presence of near-neutral

Table 4: Average ζ-potential of typical gold nanorods ($AuNR_{628}$) before and after incubating with cell medium. Values are seen to drop to nearly zero from their initial values.

Samples	$AuNR_{628}$ (mV)	PSS-$AuNR_{628}$ (mV)	PEG-$AuNR_{628}$ (mV)
Before	$+53 \pm 7.2$	-45.0 ± 3.6	-4.1 ± 0.6
After	$+5.2 \pm 2.1$	-7.0 ± 4.6	-0.3 ± 0.6

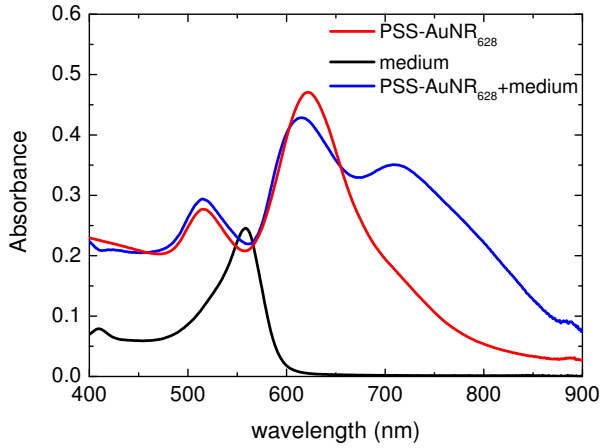

Figure 4: Optical extinction spectra of cell culture medium, and of PSS-$AuNR_{628}$ before and after incubation in the medium. A reddened broad peak appears in the spectrum pointing to flocculation or clustering.

PEG on the particle. In the case of PSS-AuNR, the presence of the anionic sulfonate groups of PSS is evident in the high negative values.

The ζ-potentials of $AuNR_{628}$ purified after incubation with the cell culture medium used are consolidated in Table 4. The original values fall to near neutral values for the CTAB-, and PSS-$AuNR_{628}$ showing compromised dispersion stability. The optical absorbance spectrum of PSS-$AuNR_{628}$ after exposure to the growth medium (Fig. 4) confirms clustering showing the appearance of a red-shifted broad peak.

3.2. Cell viability using gold nanorods

Dose response curves using products from batch $AuNR_{628}$ on cell-lines SKBR3, CHO, C2C12 and HL60 are shown in Fig. 5(a)-(d) respectively. Data points and error bars have been calculated according to eqns. 4 and 5. For all cell-lines the as-prepared and filtered AuNR resulted in 100% cell death even at the lowest concentrations. PSS-$AuNR_{628}$ gave high cell survival at low concentrations, which progressively worsened at higher concentrations for all cell-lines and particularly for HL60 cells. PEGylated nanorods evoked excellent cell survival for SKBR3, CHO and C2C12 cells for all concentrations. Only HL60 showed a toxic response at high concentrations of the PEGylated particles.

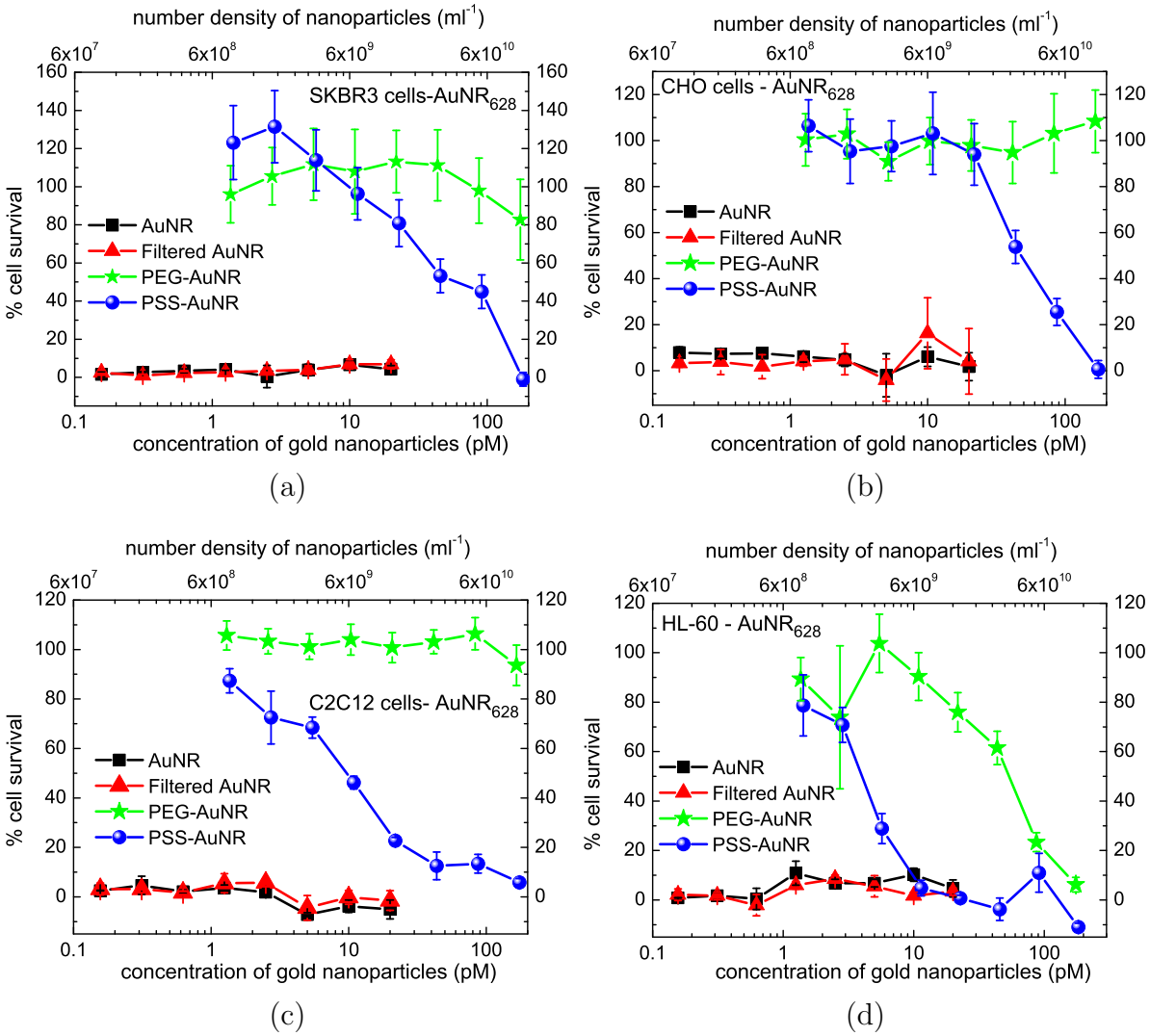

Figure 5: Dose-response curves of various cell-lines following exposure to gold nanorods (AuNR), filtered AuNR, PEGylated AuNR and PSS-treated AuNR. The results with batch $AuNR_{628}$ are shown with (a) SKBR3 cells, (b) CHO cells, (c) C2C12 cells, and (d) HL60 cells.

The median lethal concentration LC_{50} values for exposure under the tested conditions were ascertained from the dose-response curves and are consolidated in Table 5. In general CHO cells appeared to be less vulnerable to exposure to the different AuNRs compared with other cell-lines, while HL60 were most sensitive. The LC_{50} values for the PEG-$AuNR_{628}$ are indeterminate at the concentrations and exposures studied for adherent cells but are around 100 pM corresponding to a number density of 6×10^{10} NR/ml for the HL60 cells.

Similar trends were observed for the case of untreated and polymer treated-$AuNR_{773}$. (See Supplementary Fig. 1.) The LC_{50} values for PSS-coated particles showed significant differences depending on whether $AuNR_{628}$ or $AuNR_{773}$ were used; $AuNR_{628}$ has lower LC_{50} values across all cell-lines showing that the cells have higher

Table 5: The median lethal concentration LC_{50} values extracted from the dose-response curves of the tested cell-lines following exposure to gold nanorods (AuNR), filtered AuNR, PEG-AuNR and PSS-AuNR. All particles had their longitudinal plasmon peaks at 628 nm.

Cell line	AuNR pM (ml^{-1})	Filtered AuNR pM (ml^{-1})	PSS-AuNR pM (ml^{-1})	PEG-AuNR pM (ml^{-1})
SKBR3	< 0.15 (9×10^7)	< 0.15 (9×10^7)	28.4 (1.7×10^{10})	> 165 (1×10^{11})
CHO	< 0.15 (9×10^7)	< 0.15 (9×10^7)	48.5 (3×10^{10})	> 165 (1×10^{11})
C2C12	< 0.15 (9×10^7)	< 0.15 (9×10^7)	9.7 (6×10^9)	> 165 (1×10^{11})
HL60	< 0.15 (9×10^7)	< 0.15 (9×10^7)	3.0 (1.8×10^9)	103 (6×10^{10})

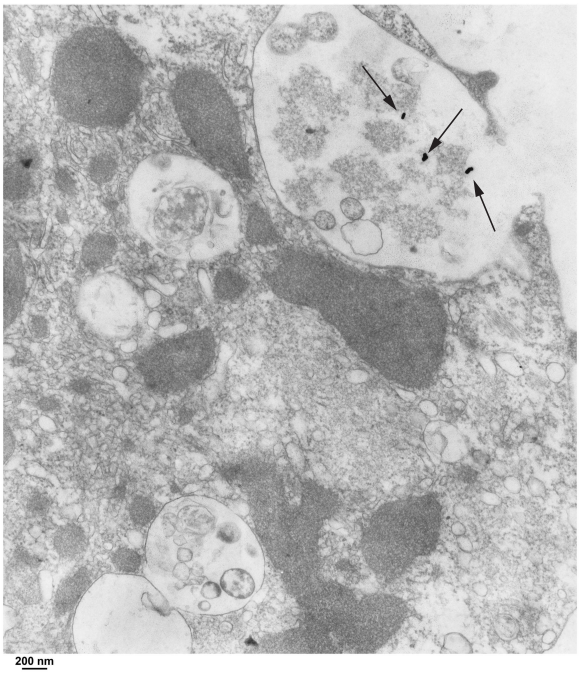

(a)

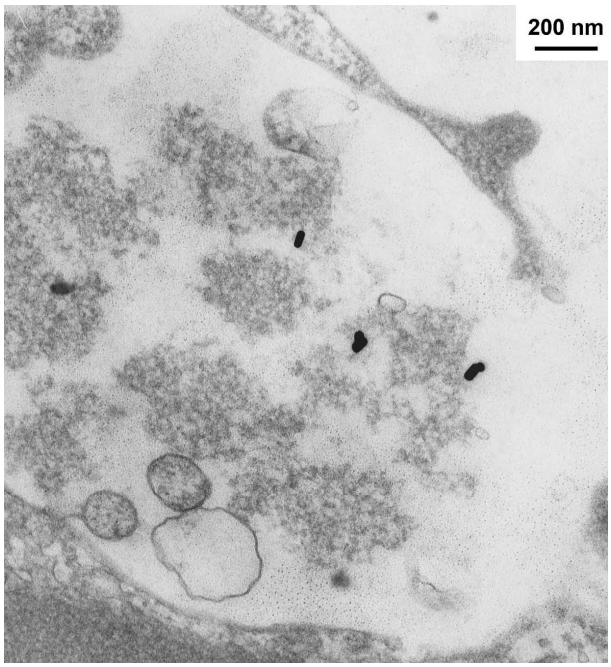

(a)

Figure 6: (a) Transmission electron micrograph of an SKBR3 cell undergoing apoptosis after exposure to PSS-$AuNR_{628}$. Gold nanorods (marked with arrows) are seen in vacuoles. (b) Zoom-in of the vacuole region showing the nanorods.

sensitivities to these particles. PEGylated particles $AuNR_{628}$ and $AuNR_{773}$ showed similar LC_{50} values on exposure to HL60 cells. (See Supplementary Table. 1.)

3.3. Electron microscopy of cellular uptake of gold nanorods

In the case of the CTAB-coated AuNRs we found cell debris, indicating massive cell death in the SKBR3 cell-line, and could not detect AuNRs in any of the left over viable cells. The PSS-AuNR samples also displayed a high degree of cell death, but still enabled the detection of AuNRs in intact, but apoptotic SKBR3 cells. The PSS-AuNRs were located a vacuole together with cell debris and/or proteins (Figure 6). Unfortunately, we were not able to determine the uptake route of these PSS-NRs. The SKBR3 cells incubated with the PEG-AuNRs, remained viable, however, no AuNRs were observed in these cells.

We did not study TEM of HL60 cells since these suffered significant cell death with exposure to the AuNRs. The HL60 cells could not be retained after sample preparation procedures, since the dead cells comprising debris were lost when they were centrifuged through the viscous plastic solution. We thus only followed nanoparticle fate using TEM in SKBR3 cells, which had shown less toxic responses following exposure to PSS-AuNR. From the cells which interacted with the particles, we were able to obtain sufficiently intact cells for imaging. We could have as well chosen to use CHO and C2C12 cells, which also show an intermediate response to the PSS-AuNR, but it was decided to use the clinically relevant SKBR3 cells.

4. Discussion

It has previously been demonstrated on a few cell-lines that excess unbound CTAB makes AuNR dispersions toxic [14, 15, 16, 17, 18] by disrupting cell membrane integrity [29]. However, CTAB is crucial for the synthesis of AuNRs: CTAB (and silver) stabilize the {110} faces of gold seed to a greater extent than the {100} surfaces leading to a faster rate of gold atom growth on the latter, consequently leading to one-dimensional growth along the [100] direction [11, 12, 13] to form rods. Further, the CTAB bilayer [28] imparts a nett positive charge to the particle and helps preserve colloidal stability by electrostatic repulsion. Thus CTAB is indispensable for low polydispersity, controllable aspect ratio [19, 30] and stability of the particles. Repeated centrifugation of AuNR can minimize free CTAB and thereby reduce toxicity. However, we found that a second cycle of centrifugation could in many cases result in irreversible aggregation of the particles. A single centrifugation following filtration gave stable AuNRs, but these were severely toxic even at the lowest concentrations of nanoparticles studied (Fig. 5).

4.1. PSS-coated gold nanorods

The model for PSS-treated particles is shown in Fig. 7(a). PSS being an anionic polyelectrolyte is electrostatically adsorbed on the positively charged CTAB bilayer. This forms an overcoat encapsulating CTAB-AuNRs. The ζ-potential values (Table 3) show a charge reversal and are evidence for this interaction. The magnitude of the ζ-potential, which is a measure of the repulsive forces present and an indicator of the

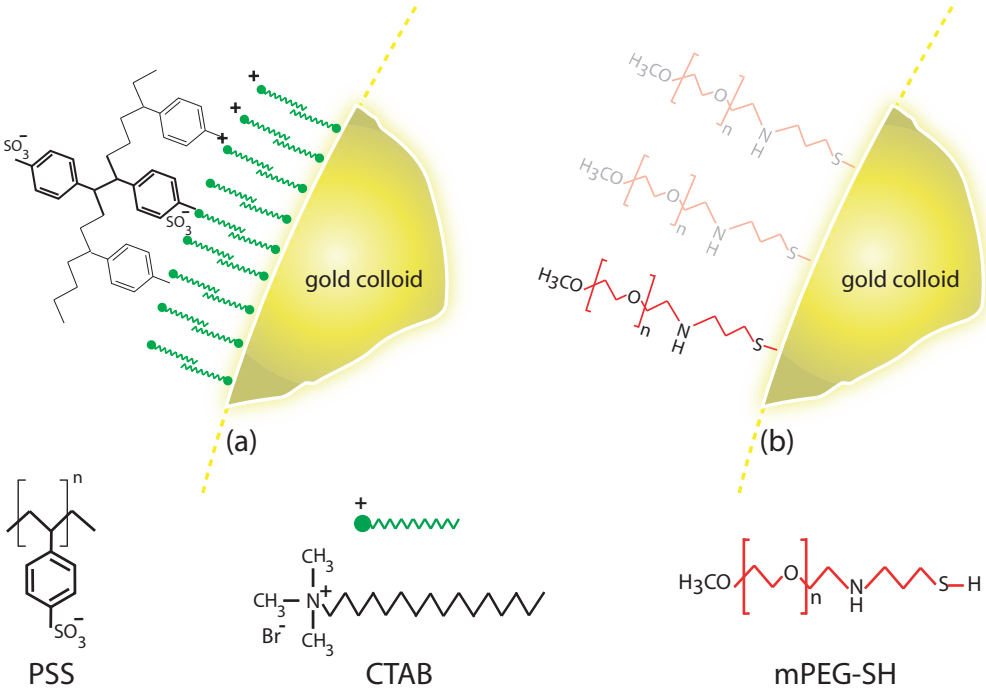

Figure 7: Models for surface modification of gold nanorods with (a) PSS, where an overcoat of the polymer occurs on the CTAB bilayer by electrostatic adsorption, (b) mPEG-SH, where sulphur-gold binding ensures replacement of the CTAB bilayer by PEG.

potential colloidal stability, is greater than the rule-of-thumb 30 mV [31]. This points to the stability of the colloidal system based on charge stabilization mechanisms, which is borne out from the largely unchanged plasmon peaks in Fig. 3(a) and (b), showing the absence of flocculation or coagulation.

Alkilany *et al* [18] showed that gold nanorods with certain polyelectrolyte surface coatings remained stable due to serum protein adsorption when incubated with cell growth medium. Our PSS-AuNRs on the other hand, suffered clustering when exposed to medium and FBS. This can be concluded from the optical spectra (Fig. 4), and from the ζ-potential values which drop to a few mV (Table 4). The presence of salts in the medium compromises charge stabilization due to electrostatic shielding. If there is sufficient protein adsorption on the particles, then the particles remain stable due to steric stabilization provided by the coating. In our case, at the concentrations chosen there appears to be inadequate adsorption of serum proteins making the AuNRs susceptible to flocculation. This has negative implications for use of such particles *in vivo*, since colloidal instability leads to loss of the predicted NR response due to two reasons. First, clustering weakens the LP peak intensity in the optical spectrum. Second, an initiation of an immune response to the agglomerates is also possible resulting in a loss of nanomaterial at target sites.

When we exposed cells to low concentrations of PSS-AuNR$_{628}$ all cell-lines showed good viability (80+%). Cell-survival worsened with progressive increase in

concentrations for three cell-lines; for HL60 cells the numbers dropped sharply to give a median LC_{50} an order of magnitude less than in the case of SKBR3 cells. The observed toxicity could be due to desorption of the PSS-CTAB complex [29] from the gold surface. This release of the toxic complex will be heightened when the particles cluster. The amount of the free complex increases with increasing concentrations and flocculation. Why HL60 cells are more affected that others is discussed further.

In the TEM images of cells exposed to PSS-$AuNR_{628}$, a few clearly affected apoptotic, but still intact, SKBR3 cells can be found with NRs present inside vacuoles. These PSS-AuNRs appear to interact with cell debris and/or proteins. We believe that although the particles are susceptible to clustering, individual NRs or smaller clusters may still enter the cell via endocytosis. We intend to investigate aspects relating to cell-death, cellular uptake and passage in more detail.

4.2. PEG-coated gold nanorods

We incubated the particles with mPEG-thiol which results in strong sulphur binding to the gold surface with replacement of (most of) the CTAB bilayer. A model of the resultant is shown in Fig. 7(b). Evidence for this is provided in the ζ-potential values for the resultant (Table. 3) which are near-neutral indicating PEG replacement of most of the CTAB. There is no compromise in colloidal stability, since the PEG layer takes over the stabilizing role of CTAB, but with a steric hindrance mechanism compared with elecrostatic or charge stabilization observed with CTAB or with the PSS-AuNR. The optical spectra (Fig. 3(a) and (b)) of the particles before and after PEGylation show that the characteristic plasmon peaks are preserved and that the colloid is stable. The particles retain excellent dispersion stability even after mixing in cell culture medium showing that the PEG-SH forms a strong link to the gold surface, and the composite is not affected by cell medium contents.

PEGylated particles elicited excellent cell viability and were essentially non-toxic for the SKBR3, CHO and C2C12 cell-lines up to concentrations of 165 pm corresponding to approximately 1×10^{11} NR/ml. HL60 cells show a linear drop in cell-survival with increasing concentrations. Since neither nanogold or PEG are themselves toxic, HL60 cell death could point to residual CTAB even after mPEG-SH treatment. However this needs to be studied in detail.

Absence of PEG-AuNR inside the intact SKBR3 cells observed using TEM suggests that PEG coatings prevent cellular uptake of the gold nanorods. In combination with the low toxicity profile (Figure 5) with the cell-line, this indicates that PEG-AuNRs have little interaction with SKBR3 cells. Huff et al [16] have also shown that cellular uptake of nanoparticles is reduced by their PEGylation.

4.3. Other remarks

The surface area of single particle of $AuNR_{628}$, calculated assuming that the NR is a hemispherically-capped cylinder and using sizes from Table 1, is 1.69 times greater

Table 6: LC_{50} values extracted from Fig. 5 and Supplementary Fig. 1, showing differences in sensitivity of the cell-lines to PSS-coated gold nanorods of two sizes.

Samples	SKBR3	CHO	C2C12	HL60
PSS-$AuNR_{628}$	28.4 pM	48.5 pM	10 pM	3 pM
PSS-$AuNR_{773}$	38 pM	57 pM	11 pM	4 pM

than for $AuNR_{773}$. The loading of the toxic CTAB bilayer is thus proportionally higher for PSS-$AuNR_{628}$ giving it a corresponding higher toxic potential than its 773 nm counterpart. This is the reason for the observed higher sensitivity of all cell-lines for exposure to PSS-$AuNR_{628}$ as assessed by LC_{50} values, compared to PSS-$AuNR_{773}$ (Table 6). In the case of PEGylated particles, surface area is not the parameter of interest for comparing cytotoxicity between the two families of NRs, since the treatment largely replaces CTAB. Indeed for the case where LC_{50} values of PEG-AuNRs are determinate, namely for HL60 cells, there was no difference in the values.

Different cells show different responses based on inherent characteristics such as surface reactivity, making a comparison across cell-lines complicated. If we take the case of PEG-AuNR exposure, HL60 cells show higher cell deaths compared with SKBR3, CHO and C2C12 cell-lines. This may be an example of such natural characteristics, making HL60 a less robust cell-line than the others. These cells divide rapidly compared to the other cell-lines, which explains their higher vulnerability to damage by the test compounds. A part of the reason may also be due to HL60 being cells in suspension. The cells expose larger surface areas compared with the two-dimensional distribution of adherent cells, with a corresponding higher probability of interaction with toxic components in the microenvironment.

Further, cell function may play a major role in determining the different responses: SKBR3 and CHO are epithelial cells. Epithelial cells, in general, line the cavities and surfaces of tissues and organs protecting the underlying tissue from mechanical injury, harmful chemicals, pathogens and excessive water loss. The lower toxicity observed in SKBR3 and CHO cells can then be attributed to this protective function.

While we have established that the biocompatibility of PEG-AuNR is superior to PSS-AuNR as manifested in the LC_{50} values, the question is whether such concentrations will ever be encountered *in vivo* at non-target sites to cause unwanted toxicity. This requires dosage studies in living organisms, where bioaccumulation of particles in organs [14] will need to be ascertained. In any case we can place the LC_{50} concentrations in context, by calculating the NR load per cell that would be *required for detection* using photoacoustic imaging. We have estimated that a cell-NR ratio of ≈ 30, marks minimum detectability using photoacoustics [32, 33]. (See Supplementary Information for details.) Compare this with the cell-NR ratio of 360,000 calculated at the LC_{50} for PSS-$AuNR_{628}$ with HL60 cells.

5. Conclusions

The implication of this study on utilization is that PEGylated AuNRs are superior to PSS-coated AuNRs from the point of view of biocompatibility. Treating the particles with mPEG-SH, replaces toxic CTAB with PEG, and also renders the particles colloidally stable even in the presence of salts in cell culture medium. Treatment with PSS and possibly other polyelectrolytes, is an inferior detoxification approach since the polymer only encapsulates the AuNR with its CTAB bilayer intact. PSS-AuNRs cluster and coagulate on exposure to cell culture medium, which will further hamper future use *in vivo*. This *in vitro* study is valuable in learning about necessary modifications to AuNRs in a quick and relatively inexpensive way to improve biocompatibility. Ultimately we intend to test these particles *in vivo* with all the complexity of blood flow, immunological and inflammatory responses, and the biological variability inherent to such systems [34]. Another direction which is being explored is to use PEG not only to detoxify and stabilize the AuNRs, but also as a linker to attach appropriate antibodies at their free ends.

6. Acknowledgements

This work is funded through the thrust area program NIMTIK of the University of Twente; through the PRESMITT project (IPD067771) of the SenterNovem program IOP Photonic Devices; and by the Nederlandse Wetenschappelijk Organisatie (NWO) and Stichting Technische Wetenschappen (STW) through project TTF 6527; and by a KWF-translational research award (Grant No. PGF 2009-4344; FvL)

References

[1] West J L and Halas N J 2003 Engineered nanomaterials for biophotonics applications: Improving sensing, imaging, and therapeutics *Ann. Rev. Biomed. Engg.* **5** 285

[2] Liao H, Nehl C L and Hafner J H Biomedical applications of plasmon resonant metal nanoparticles *Nanomedicine* **1**

[3] Murphy C J, Sau T K, Gole A M, Orendorff C J, Gao J, Gou L, Hunyadi S E and Li T 2005 Anisotropic metal nanoparticles: Synthesis, assembly, and optical applications *J. Phys. Chem. B* **109** 13857

[4] Huang X, El-Sayed I H, Qian W and El-Sayed M A 2006 Cancer cell imaging and photothermal therapy in the near-infrared region by using gold nanorods *J. Am. Chem. Soc.* **128** 2115

[5] Eustis S and El-Sayed M A Why gold nanoparticles are more precious than pretty gold: Noble metal surface plasmon resonance and its enhancement of the radiative and nonradiative properties of nanocrystals of different shapes

[6] Eghtedari M, Oraevsky A A, Copland J A, Kotov N A, Conjusteau A and Motamedi M 2007 High sensitivity of in vivo detection of gold nanorods using a laser optoacoustic imaging system *Nano Lett.* **7** 1914

[7] Oldenburg A L, Hansen M N, Ralston T S, Wei A and Boppart S A 2009 Imaging gold nanorods in excised human breast carcinoma by spectroscopic optical coherence tomography *J. Mater. Chem*

[8] Huang X, Jain P K, El-Sayed I H and El-Sayed M A 2007 Gold nanoparticles: interesting optical properties and recent applications in cancer diagnostics and therapy *Nanomedicine* **2** 681
[9] Tromberg B J, Shah N, Lanning R, Cerussi A, Espinoza J, Pham T, Svaasand L and Butler J 2000 Non-invasive in vivo characterization of breast tumors using photon migration spectroscopy *Neoplasia* **2** 2640
[10] Lewinski N, Colvin V and Drezek R 2008 Cytotoxicity of nanoparticles *Small* **4** 26
[11] Liu M and Guyot-Sionnest P 2005 Mechanism of silver(i)-assisted growth of gold nanorods and bipyramids *J. Phy. Chem. B* **109** 22192
[12] Orendorff C J and Murphy C J 2006 Quantitation of metal content in the silver-assisted growth of gold nanorods *J. Phys. Chem. B* **110** 3990
[13] Grzelczak M, Prez-Juste J, Mulvaney P and Liz-Marzán L M 2008 Shape control in gold nanoparticle synthesis *Chem. Soc. Rev.* **37** 1783
[14] Nidome T, Yamagata M, Okamoto Y, Akiyama Y, Takahashi H, Kawano T, Katayama Y and Niidome Y 2006 Peg-modified gold nanorods with a stealth character for in vivo applications *J. Contl. Release* **114** 343
[15] Takahashi H, Niidome Y, Niidome T, Kaneko K, Kawasaki H and Yamada S 2006 Modification of gold nanorods using phosphatidylcholine to reduce cytotoxicity *Langmuir* **22** 2
[16] Huff T B, Hansen M N, Zhao Y, Cheng J X and Wei A 2007 Controlling the cellular uptake of gold nanorods *Langmuir* **23** 1596
[17] Hauck T S, Ghazani A A and Chan W C W 2008 Assessing the effect of surface chemistry on gold nanorod uptake, toxicity, and gene expression in mammalian cells *Small* **4** 153
[18] Alkilany A M, Nagaria P K, Hexel C R, Shaw T J, Murphy C J and Wyatt M D 2009 Cellular uptake and cytotoxicity of gold nanorods: Molecular origin of cytotoxicity and surface effects *Small* **5** 701
[19] Nikoobakht B and El-Sayed M A 2003 Preparation and growth mechanism of gold nanorods (nrs) using seed-mediated growth method *Chem. Mater.* **15** 1957
[20] Alekseeva A V, Bogatyrev V A, Dykman L A, Khlebtsov B N, Trachuk L A, Melnikov A G and Khlebtsov N G 2005 Preparation and optical scattering characterization of gold nanorods and their application to a dot-immunogold assay *Appl. Opt.* **44** 6285
[21] Rayavarapu R, Petersen W, Ungureanu C, Post J, van Leeuwen T and Manohar S 2007 Synthesis and bioconjugation of gold nanoparticles as potential molecular probes for light-based imaging techniques *Int. J. Biomed. Imaging* **29817** 29817
[22] Connor E E, Mwamuka J, Gole A, Murphy C J and Wyatt M D 2005 Gold nanoparticles are taken up by human cells but do not cause acute cytotoxicity *Small* **1** 325
[23] Draine B T and Flatau P J 1994 Discrete-dipole approximation for scattering calculations *J. Opt. Soc. Am. A* **11** 1491
[24] Ungureanu C, Rayavarapu R G, Manohar S and Van Leeuwen T G 2009 Discrete dipole approximation simulations of gold nanorod optical properties: Choice of input parameters and comparison with experiment *J. Appl. Phys.* **105** 102032
[25] Manohar S, Kharine A, Van Hespen J C G, Steenbergen W and Van Leeuwen T G 2005 The twente photoacoustic mammoscope *Phys. Med. Biol.* **50** 25432557
[26] Manohar S, Vaartjes S E, Van Hespen J C G, Klaase J M, Van den Engh F M, Steenbergen W and Van Leeuwen T G 2007 Initial results of *in vivo* non-invasive cancer imaging in the human breast using near-infrared photoacoustics *Opt. Express* **15** 12277
[27] Lyons L 1991 *A practical guide to data analysis for physical science students* Cambridge University Press, New York
[28] Nikoobakht B and El-Sayed M A 2001 Evidence for bilayer assembly of cationic surfactants on the surface of gold nanorods *Langmuir* **17** 6368
[29] Leonov A P, Zheng J, Clogston J D, Stern S T, Patri A K and Wei A 2008 Detoxification of gold nanorods by treatment with polystyrenesulfonate *ACS Nano* **2** 2481
[30] Gao J, Bender C M and Murphy C J 2003 Dependence of the gold nanorod aspect ratio on the

nature of the directing surfactant in aqueous solution *Langmuir* **19** 9065
[31] Malvern Instruments Ltd. Worcestershire, UK 2008 *Malvern Zetasizer Manual*
[32] Jose J, Willemink R, Resink S, Maalderink T, van Hespen J C G, Van Leeuwen T G and Manohar S 2009 Ultrasound-transmission parameter imaging in a photoacoustic imager volume 7371 73710S SPIE
[33] Jose J, Maalderink T, Willemink G H, Van Neck J W, Manohar S and Van Leeuwen T G A Computed Tomography photoacoustic imager for imaging murine disease models *in prep*
[34] Panessa-Warren B J, Warren J B, Maye M M and Schiffer W 2009 *Nanoparticles and Nanodevices in Biological Applications: The INFN Lectures - Vol I* chapter Nanoparticle Interactions with Living Systems: In Vivo and In Vitro Biocompatibility, 1–46 Springer-Verlag, Heidelberg

Supplementary Information: *In vitro* toxicity studies of polymer-coated gold nanorods

Raja G. Rayavarapu[1,*], Wilma Petersen[1,*], Liesbeth Hartsuiker[2], Patrick Chin[3], Hans Janssen[4], Fijs W. B. van Leeuwen[3], Cees Otto[2], Srirang Manohar[1,§] and Ton G. van Leeuwen[1,5]

[1]*Biomedical Photonic Imaging Group, MIRA Institute for Biomedical Technology and Technical Medicine, Faculty of Science and Technology, University of Twente, P.O. Box 217, 7500AE Enschede, The Netherlands.*

[2]*Medical Cell Biophysics, MIRA Institute for Biomedical Technology and Technical Medicine, Faculty of Science and Technology, University of Twente, P.O. Box 217, 7500AE Enschede, The Netherlands*

[3]*Division of Diagnostic Oncology, The Netherlands Cancer Institute, 1066 CX Amsterdam, The Netherlands.*

[4]*Division of Cell Biology, The Netherlands Cancer Institute, 1066 CX Amsterdam, The Netherlands.*

[5]*Biomedical Engineering and Physics, Academic Medical Center, University of Amsterdam, PO Box 22700, 1100 DE Amsterdam, The Netherlands.*

[*]*These authors contributed equally* [§]*Correspondence: s.manohar@utwente.nl*

Detailed protocol for the synthesis of gold nanorods ($AuNR_{628}$ and $AuNR_{773}$) using seed-mediated silver-assisted surfactant method

Step 1: Synthesis of CTAB-stabilized Au seed

An aqueous solution of CTAB (0.2 M) is prepared by sonication for 40 minutes at 45˚C in a water bath. Gold salt $HAuCl_4.3H_2O$ (5 ml; 0.0005 M) is added to the CTAB (5 ml; 0.2 M) with continuous stirring. A freshly prepared, ice-cold, aqueous solution of

$NaBH_4$ (0.6 ml; 0.01 M) is added to the resultant, all at once, with vigorous stirring. The seed solution appears light brownish in colour.

Step 2: Preparation of growth solution

Ten identical flasks containing growth solutions are prepared, which are at the last stage pooled together to obtained increased volumes/concentrations. Each growth solution consists of CTAB (5 ml; 0.2 M) and $HAuCl_4.3H_2O$ (5 ml; 0.001 M). To synthesize nanorods with longitudinal plasmon peaks (LP) at 628 nm ($AuNR_{628}$), 50 µl $AgNO_3$ (0.006 M) is added to the growth solutions. To achieve $AuNR_{773}$ particles, 200 µl $AgNO_3$ (0.006 M) is added. Following this, 60 µl of ascorbic acid (0.1 M) is added to each flask to give colourless solutions.

Step 2: Growth phase

14 µl of the CTAB-capped seed solution prepared above, is added to each growth solution in the flasks and the resultants gently mixed. The seed solution should be used within 5-10 minutes of preparation. The resultants are maintained undisturbed at 27 ˚C for 24 hours, during which time the nanorods are formed. These AuNR solutions are centrifuged at 10000 g/20 minutes to remove excess of CTAB, and the pellets of AuNR are added together to increase the concentration of particles. The resulting pellet is dispersed in 1X PBS. The final volume of AuNR is around 100 ml, with concentrations approaching $1x10^{11}$ NRs/ml.

Cell viability on exposure to $AuNR_{773}$

Dose response curves of cell-lines SKBR3, CHO, C2C12 and HL60 exposed to $AuNR_{773}$ are shown in Supplementary Fig. 1. Data points and error bars are calculated according to manuscript eqns. 4 and 5. Similar trends as in the case of exposure to $AuNR_{628}$ are seen.

For all cell-lines the as-prepared and filtered AuNR resulted in 100% cell death even at the lowest concentrations. PSS-AuNR$_{773}$ gave high cell survival at low concentrations, which progressively worsened at higher concentrations for all cell-lines and particularly for HL60 cells. PEG-AuNR$_{773}$ shows excellent cell survival for all but HL60 cells.

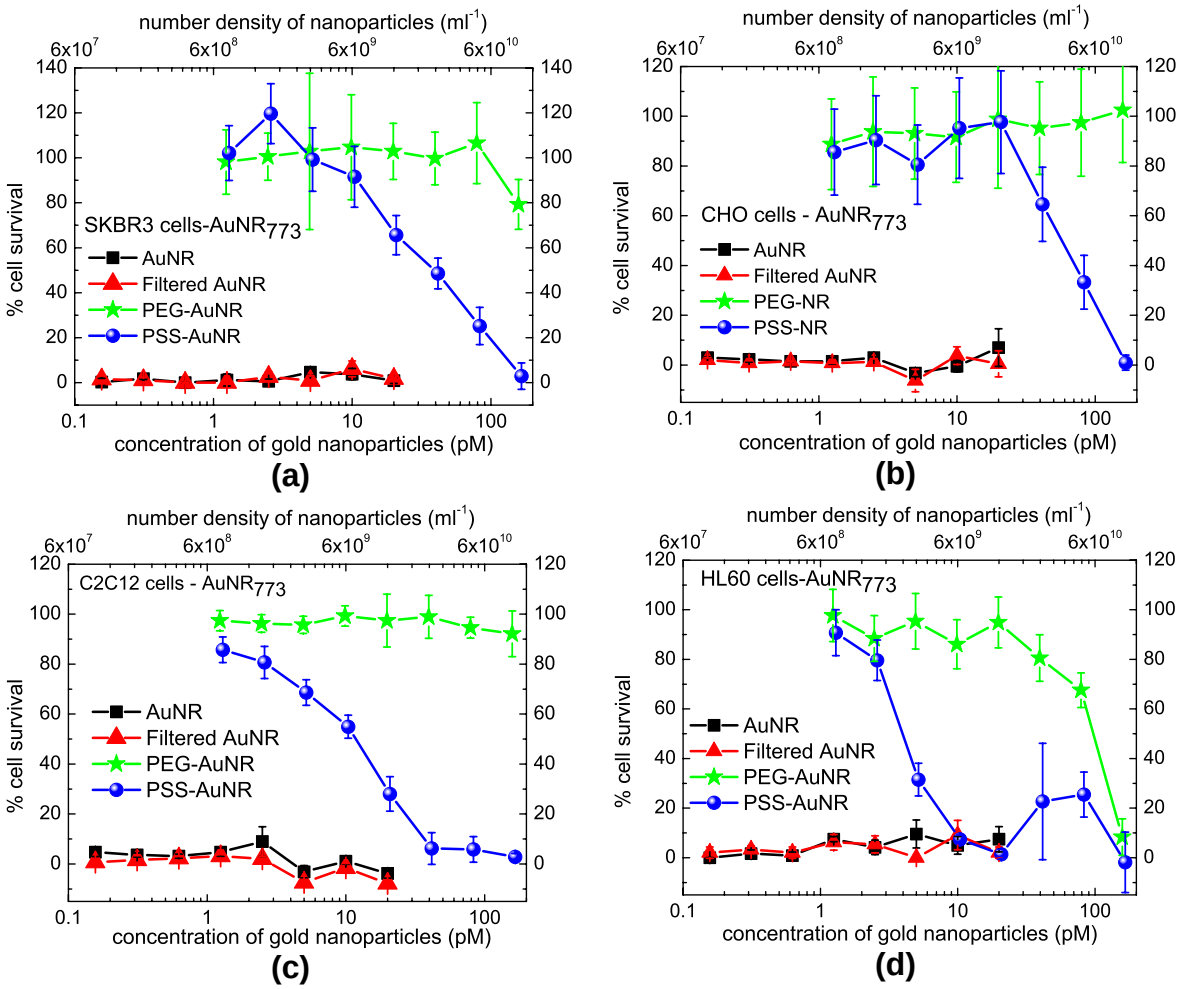

Supplementary Figure 1: Dose-response curves of various cell-lines following exposure to various gold nanorods having longitudinal plasmon peak at 773 nm. Particles studied are AuNR$_{773}$, filtered AuNR$_{773}$, PEGylated AuNR$_{773}$ and PSS-treated AuNR$_{773}$. Cells used are (a) SKBR3 cells, (b) CHO cells, (c) C2C12 cells, and (d) HL60 cells.

The median lethal concentration LC$_{50}$ values for exposure under the tested conditions were ascertained from Supplementary Fig. 1(a)-(d) and are consolidated in Supplementary Table 1. The values for PEG-AuNR$_{773}$ are indeterminate at the

concentrations and exposures studied for adherent cells but are around 100 pm corresponding to a number density of $6x10^{10}$ NR/ml for the HL60 cells.

Supplementary Table 1: LC50 values in pM of unmodified and surface modified $AuNR_{773}$ particles. LC50 values are determined from the dose-response curves as the concentration where there is 50% cell death.

Cell line	$AuNR_{773}$ (pm)	Filtered-$AuNR_{773}$ (pm)	PSS-$AuNR_{773}$ (pm)	PEG-$AuNR_{773}$ (pm)
SKBR3	< 0.1563	< 0.1563	38	> 157
CHO	< 0.1563	< 0.1563	57	> 157
C2C12	< 0.1563	< 0.1563	11	> 157
HL60	< 0.1563	< 0.1563	4	97

Comparison of LC_{50} concentrations with AuNR concentrations required for photoacoustic imaging

The LC_{50} values obtained may be compared with requirements of AuNR concentrations for the specific application of photoacoustic imaging. Recently we have determined using our photoacoustic Computed Tomography (CT) mouse imager [1,2] that the system is capable of detecting $3.3x10^{10}$ NR/ml in a 2 mm diameter alginate sphere. The NR-embedded sphere functioned as an inhomogeneity, embedded at the center of a 26 mm diameter cylindrical, tissue-mimicking phantom [3,4]. The concentration corresponds to a number of $138x10^6$ NRs in the sphere. In tissue, this volume would be occupied by approximately $5x10^6$ cells – cells represented by spheres of 10 μm diameter. Under the assumption that a similar concentration would also be possible in tissue, the ratio of cells to NRs would be ≈ 30. This figure is considerably lower than the cell-NR ratios encountered in this study. For example, HL60 cells (5000

cells) to PSS-AuNR$_{628}$ ($1.8x10^9$ NR/ml) exposure at the LC_{50} value yield a cell-NR ratio of 360,000.

References

[1] J. Jose, R. Willemink, S. Resink, T. Maalderink, J. C. G. van Hespen, T. G. Van Leeuwen, and S. Manohar, "Ultrasound-transmission parameter imaging in a photoacoustic imager," *Novel Optical Instrumentation for Biomedical Applications IV* 7371(1), p. 73710S, SPIE, 2009.
[2] J. Jose, T. Maalderink, G. H. Willemink, J. W. Van Neck, S. Manohar, and T. G. Van Leeuwen, "A Computed Tomography photoacoustic imager for imaging murine disease models," *in prep*.
[3] A. Kharine, S. Manohar, R. Seeton, R. G. M. Kolkman, R. A. Bolt, W. Steenbergen and F. F. M. de Mul, "Poly(vinyl alcohol) gels for use as tissue phantoms in photoacoustic mammography," *Phys. Med. Biol.* 48, 357, 2003.
[4] S. Manohar, A. Kharine, J. C. G. van Hespen, W. Steenbergen and T. G. van Leeuwen, "Photoacoustic mammography laboratory prototype: imaging of breast tissue phantoms," *J Biomed Opt.* 9, 1172, 2004.
